2017

Conformational changes at cytoplasmic intersubunit interactions control Kir channel gating

Shizhen Wang
Washington University School of Medicine in St. Louis

William F. Borschel
Washington University School of Medicine in St. Louis

Sarah Heyman
Washington University School of Medicine in St. Louis

Phillip Hsu
Washington University School of Medicine in St. Louis

Colin G. Nichols
Washington University School of Medicine in St. Louis

Conformational changes at cytoplasmic intersubunit interactions control Kir channel gating

Received for publication, March 10, 2017, and in revised form, April 17, 2017 Published, Papers in Press, April 26, 2017, DOI 10.1074/jbc.M117.785154

Shizhen Wang, William F. Borschel[1], Sarah Heyman, Phillip Hsu, and Colin G. Nichols[2]

From the Department of Cell Biology and Physiology and the Center for the Investigation of Membrane Excitability Diseases, Washington University School of Medicine, St. Louis, Missouri 63110

Edited by F. Anne Stephenson

The defining structural feature of inward-rectifier potassium (Kir) channels is the unique Kir cytoplasmic domain. Recently we showed that salt bridges located at the cytoplasmic domain subunit interfaces (CD-Is) of eukaryotic Kir channels control channel gating via stability of a novel inactivated closed state. The cytoplasmic domains of prokaryotic and eukaryotic Kir channels show similar conformational rearrangements to the common gating ligand, phosphatidylinositol bisphosphate (PIP_2), although these exhibit opposite coupling to opening and closing transitions. In Kir2.1, mutation of one of these CD-I salt bridge residues (R204A) reduces apparent PIP_2 sensitivity of channel activity, and here we show that Ala or Cys substitutions of the functionally equivalent residue (Arg-165) in the prokaryotic Kir channel KirBac1.1 also significantly decrease sensitivity of the channel to PIP_2 (by 5–30-fold). To further understand the structural basis of CD-I control of Kir channel gating, we examined the effect of the R165A mutation on PIP_2-induced changes in channel function and conformation. Single-channel analyses indicated that the R165A mutation disrupts the characteristic long interburst closed state of reconstituted KirBac1.1 in giant liposomes, resulting in a higher open probability due to more frequent opening bursts. Intramolecular FRET measurements indicate that, relative to wild-type channels, the R165A mutation results in splaying of the cytoplasmic domains away from the central axis and that PIP_2 essentially induces opposite motions of the major β-sheet in this channel mutant. We conclude that the removal of stabilizing CD-I salt bridges results in a collapsed state of the Kir domain.

Eukaryotic inward-rectifier potassium (Kir)[3] channels are expressed in many tissues, including heart, skeletal muscle, kidney, cochlea, glia, neurons, retina, pancreas, small intestine, and stomach, and are essential for regulation of excitability and maintenance of cellular potassium homeostasis (1, 2). Mutations of Kir channels have been associated with multiple diseases, ranging from cardiac failure to renal, ocular, pancreatic, and neurological abnormalities (3–5). All eukaryotic Kir channels require phosphatidylinositol 4,5-bisphosphate (PIP_2), a direct regulator of many other ion channels (6, 7), for activation. Crystal structures of eukaryotic Kir channels in complex with PIP_2 have revealed the PIP_2 binding pockets (8, 9) and have also indicated structural rearrangements associated with gating, including rigid-body motions of the cytoplasmic domain coupled to TM2 bending and/or formation of a tethering helix that pulls the cytoplasmic domain toward membrane surface (8, 9).

Many disease-causing mutations are located in the cytoplasmic domain of Kir channels where multiple regulators, such as protons, sodium, ATP, and G-protein $\beta\gamma$ subunits bind (1, 2, 10–14). However, molecular mechanisms that couple ligand binding to conformational changes and intersubunit interactions of the cytoplasmic domain are still unclear. As a bacterial homologue (15–17), KirBac1.1 is missing three critical residues in each of the linking strands between the cytoplasmic domain and the transmembrane domain (8, 18, 19). These strands are directly involved in PIP_2 binding in eukaryotic Kir channels (8, 18, 19). Hence KirBac1.1 has a distinct PIP_2-binding pocket structure and differential gating responses to PIP_2 in comparison with eukaryotic Kir channels (20): eukaryotic Kir channels are opened by PIP_2, but KirBac1.1 is closed in the presence of PIP_2. Utilizing intramolecular FRET approaches, our previous work has revealed motions of the KirBac1.1 cytoplasmic domain associated with PIP_2-dependent channel gating (12, 22). This leads to a proposed gating mechanism that is consistent with models of channel gating based on KirBac3.1 and Kir3.2 crystal structures but with opposite gating consequences upon PIP_2 binding between the prokaryotic and eukaryotic channels (9, 22, 23).

We recently showed that conserved salt bridges in the cytoplasmic domain interface (CD-I) stabilize a PIP_2-accessible conformation of eukaryotic Kir channels and that breaking these salt bridges results in stabilization of a PIP_2-inaccessible "inactivated" closed state (24). In the present work we show that breaking of the CD-I salt bridge by the R165A mutation stabilizes open KirBac1.1 channels also by reducing apparent PIP_2 sensitivity. We examined the structural changes that accom-

This work was supported by National Institutes of Health Grant HL54171 (to C. G. N.). The authors declare that they have no conflicts of interest with the contents of this article. The content is solely the responsibility of the authors and does not necessarily represent the official views of the National Institutes of Health.

[1] Supported by National Institutes of Health Training Grants DK007120-38, HL007275-35, and HL125241-01.

[2] To whom correspondence should be addressed: Dept. of Cell Biology and Physiology, Washington University School of Medicine, 660 South Euclid Ave., St. Louis, MO 63110. Tel.: 314-362-6630; Fax: 314-362-7463; E-mail: cnichols@wustl.edu.

[3] The abbreviations used are: Kir, inward-rectifier potassium; PIP_2, phosphatidylinositol 4,5-bisphosphate; CD-I, cytoplasmic domain interface; P_o, open probability; POPE, 1-palmitoyl-2-oleyl-*sn*-glycero-3phosphoethanolamine; POPG, 1-palmitoyl-2-oleyl-*sn*-glycero-3-phosphoglycerol); MTS, methyl thiosulfhydryl; EDANS, (5-((2-aminoethyl)amino)naphthalene-1-sulfonic acid); DABCYL- 4-((4-(dimethylamino)phenyl)azo)benzoic acid.

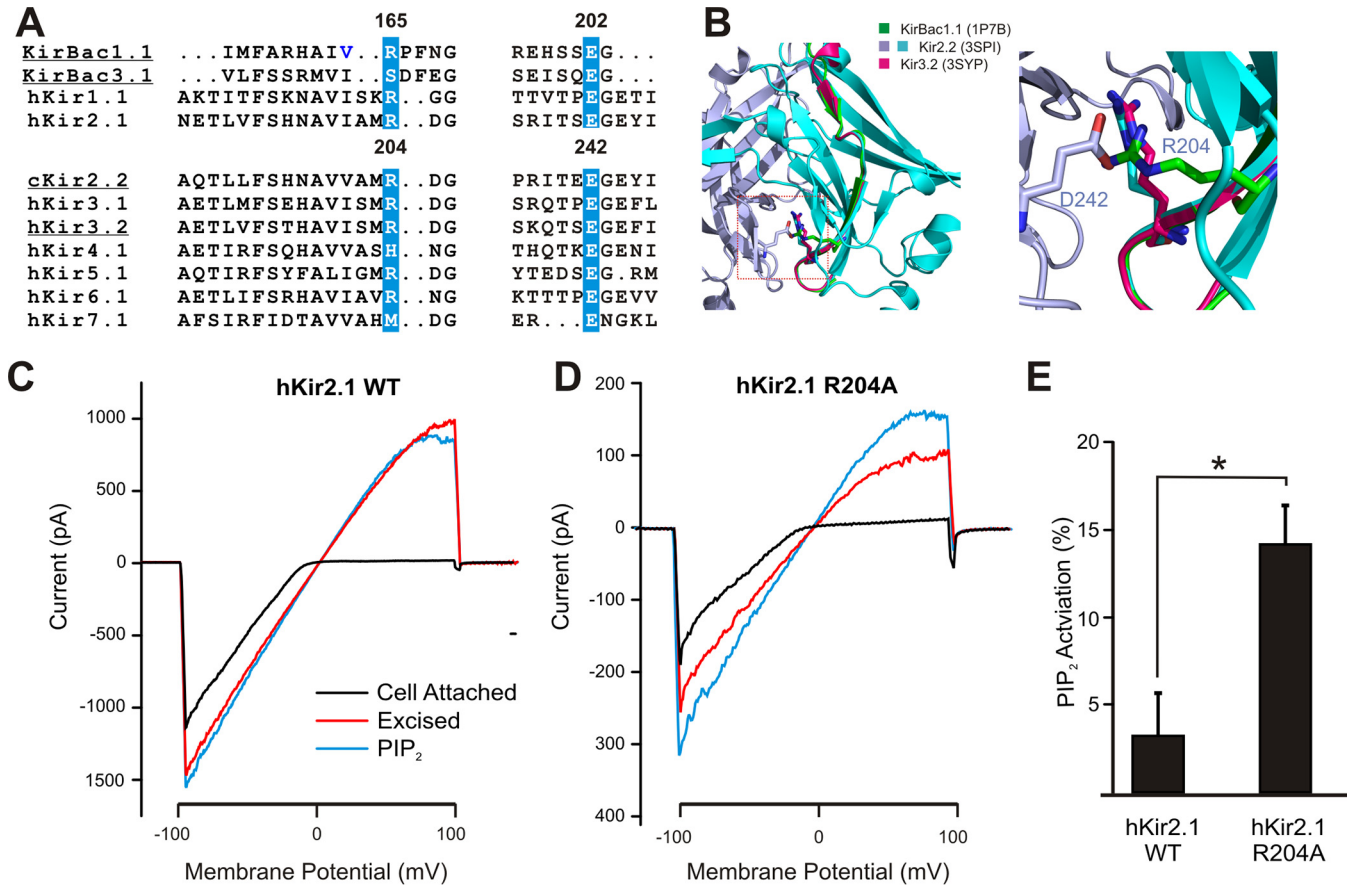

Figure 1. The R204A mutation reduced PIP_2 sensitivity of Kir2.1. *A*, sequence alignments of Kir channels using ClustalW; a two-residue gap was introduced to comply with the structural alignments. *B*, Kir channel cytoplasmic domains of KirBac1.1 (PDB code 2WLL, *green*), Kir3.2 (3SYP, *pink*) and Kir2.2 (3SPI, *cyan* and *light blue*) were aligned with PyMOL, with Arg-165 of KirBac1.1 and equivalent Arg-215 of Kir3.2, and Arg-204 of Kir2.2 highlighted in the *right panel as sticks*. *C* and *D*, representative macroscopic currents of human Kir2.1 WT (*C*) and R204A (*D*) mutants in cell-attached and excised (inside-out) patches in response to a voltage ramp from −100 to +100 mV membrane potential; 4.6 μM μM PIP_2 was applied in the bath solution after the patches were excised and the currents reached steady state. *E*, changes of Kir2.1 WT and R204A channel currents induced by 4.6 μM PIP_2. Channel potentiation by PIP_2 was calculated using equation $\% = I_{PIP2}/I_{Excised} - 1$, where $I_{Excised}$ is the steady-state current at −100 mV in excised mode, and I_{PIP2} is the steady-state current after PIP_2 addition. WT, $n = 6$; Arg-204, $n = 5$; *, $p < 0.05$.

pany this mutation by intramolecular FRET measurements. The data lead us to conclude that CD-I stabilization by the Arg-165–Glu-202 salt bridge (or equivalent salt bridge in eukaryotic Kir channels) stabilizes a tight conformation of the tetrameric Kir channel domains that is PIP_2-accessible, which results in higher open probability of eukaryotic Kir channels and lower activity of KirBac channels.

Results

An arginine residue at the cytoplasmic intersubunit interface modified PIP_2 sensitivity of Kir2.1

As shown in crystal structures of Kir2.2 and Kir3.2 (8, 9, 25), Kir2.1 residue Arg-204, located in the interface between cytoplasmic domains (CD-I) forms a salt bridge with Glu-241 of the adjacent subunit. These charged residues are highly conserved throughout both prokaryotic and eukaryotic Kir channels (Fig. 1, *A* and *B*), and disruption of this salt bridge reduces the open probability (P_o) of Kir2.1 and Kir6.2 channels by induction of a PIP_2-inaccessible inactivated closed state (26). At the ambient PIP_2 levels in membranes from cell lines such as COSm6 (27, 28), recombinant Kir2.1 channels exhibit a high P_o (~0.95) that is only slightly enhanced by additional cytoplasmic PIP_2 (Fig. 1*C*). Kir2.1[R204A] mutant channels exhibit lower channel activity than wild type (WT) in excised patches but are then significantly more activated by similar exposure to PIP_2 (Fig. 1, *D* and *E*), indicating a reduced apparent PIP_2 sensitivity and reflecting the stabilization of the inactivated state by this mutation (24).

The equivalent Arg-165 of prokaryotic KirBac1.1 also reduced sensitivity to PIP_2

In contrast to the activating effect of PIP_2 on Kir2.1, prokaryotic KirBac1.1 is strongly inhibited by PIP_2, assessed using Rb efflux from liposomes with or without PIP_2 (Fig. 2*A*) (19). The R165C mutation significantly diminishes KirBac1.1 channel inhibition by PIP_2 (Fig. 2*A*), although sensitivity can be restored by modifying the cysteine with MTS reagents carrying positive, but not negative charged groups (Fig. 2*A*). We examined the effect of additional substitutions at residue 165. Although introduction of the charge-maintaining R165K mutation did not affect PIP_2 sensitivity, neutralization to either R165A or R165C significantly reduced PIP_2 sensitivity (Fig. 2*B*). Although not fully resolved in the available KirBac1.1 crystal structure (16), structural alignments indicate that the side chain of Arg-

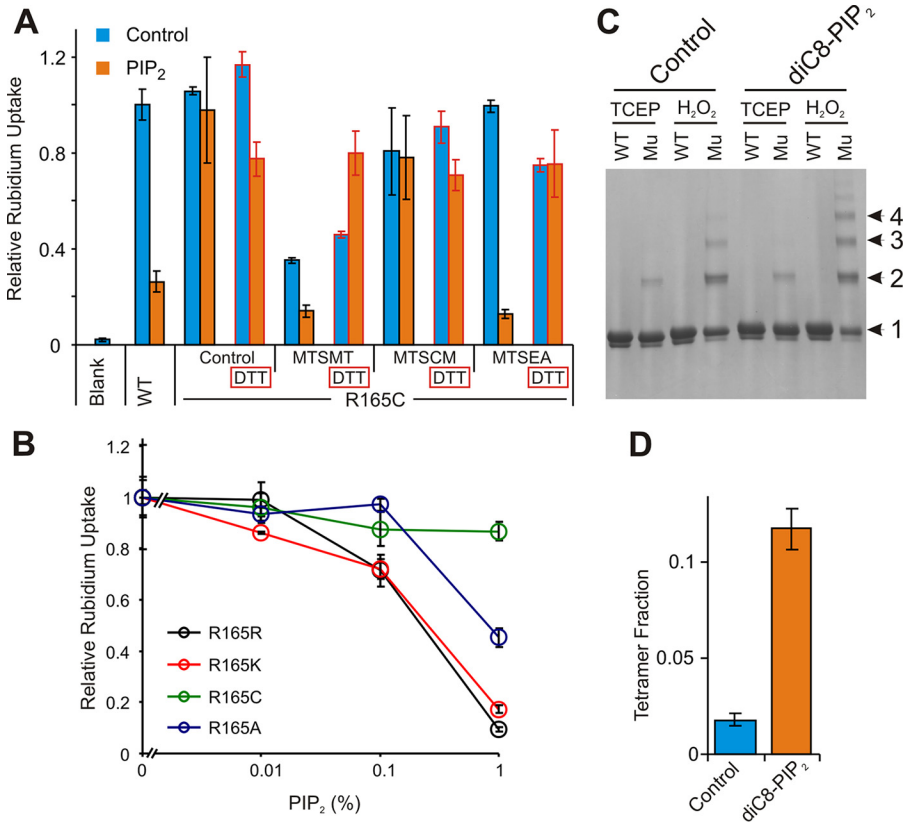

Figure 2. The equivalent Arg-165 of KirBac1.1 determined its PIP_2 sensitivity. *A*, MTS reagents with positive charged group reversibly modify the sensitivity of KirBac1.1-R165C to PIP_2. Purified KirBac1.1-R165C in buffer containing 20 mM Hepes, 150 mM KCl, and 5 mM DM, pH 7.5, was modified by MTSMT, MTSCM, and MTSEA (protein:MTS-reagents = 1:10) at room temperature for 30 min, then reconstituted into liposomes (POPE:POPG = 3:1) with or without 1% of PIP_2; the MTS- modification was removed by 25 mM DTT treatment at room temperature for 30 min. *B*, mutational analysis of the role of Arg-165 in determining the PIP_2 sensitivity of KirBac1.1. Purified KirBac1.1-R165X mutants were reconstituted into liposomes (POPE:POPG = 3:1) containing 0.0, 0.01, 0.1, or 1.0% of PIP_2. The relative rubidium uptake at different PIP_2 concentrations was determined and normalized as that described under "Experimental Procedures" (mean ± S.E., $n = 3$ in each case). *C*, SDS-PAGE analysis of disulfide bond formation between intersubunit R165C and E202C. Monomer, dimer, trimer, and tetramer bands were marked by *arrows*. KirBac1.1 WT and R165C-E202C mutant (*Mu*) in the presence and absence of 75 μM diC8-PIP_2 were treated with 5 mM H2O2 or tris(2-carboxyethyl)phosphine (*TCEP*) for 3 h under room temperature. *D*, densitometry was performed on scanned gel images with ImageJ software, and the tetramer fraction was calculated as density ratio of the tetrameric band to all oligomeric bands in the same lane.

165 normally forms a salt bridge with Glu-202 in the neighboring subunit (Fig. 1*B*) (16). A double cysteine (R165C/E202C) mutant was constructed and purified to test potential for physical connection between residues Arg-165 and Glu-202 in KirBac1.1. Interestingly, the KirBac1.1 E202C mutant does not express a protein that could be purified, but expression is rescued by introducing the additional R165C mutation. In addition, WT KirBac1.1 runs almost completely as a monomer in SDS-PAGE, but the R165C/E202C double mutant showed a clear dimeric band in oxidizing conditions (Fig. 2*B*) indicating formation of an intersubunit R165C–E202C disulfide bridge, reflecting close proximity of the two residues in the intact tetramer. Moreover, these multimer bands were more prominent in the presence of diC8-PIP_2 (Fig. 2. *B* and *C*), implying that the Arg-165–Glu-202 bridge may be stabilized in the PIP_2-driven closed state of the KirBac1.1 channel. Functional and structural conservation of the Arg-165–Glu-202 and equivalent salt bridges in both prokaryotic and eukaryotic Kir channels (24) allows us to investigate the structural role of intersubunit interactions in controlling Kir channel gating generally using KirBac1.1 as a model.

Stoichiometric effect of Arg-165–Glu-202 bridges on PIP_2 sensitivity of KirBac1.1

Kir channels are tetrameric proteins. To gain insight to the number of Arg-165–Glu-202 bridges within a tetramer that are required to maintain PIP_2 sensitivity, we generated tandem KirBac1.1 constructs, which permits introduction of different numbers of R165A mutations in different configurations within the functional channel. Gel filtration profiles show that all such concatemeric proteins exist primarily as tetramers (Fig. 3*A*). Tandem dimeric or tetrameric KirBac1.1 appear as dimer or tetramer bands, respectively, in SDS-PAGE (Fig. 3*B*) together with some lower oligomer bands presumably resulting from linker degradation. The tandem dimer KirBac1.1 channel, with two R165A mutations at diagonally opposed subunits within the tetramer, shows even higher PIP_2 sensitivity than WT, implying that a conformation with 2-fold symmetry, as is present in KirBac3.1 crystal structures, may favor channel closure (29). By contrast, a tandem tetramer construct with two adjacent R165A mutations became markedly less PIP_2 sensitive, and KirBac1.1 tetramers with either three or four R165A mutations (Fig. 3*B*) were equally PIP_2 insensitive (Fig. 3*C*). These

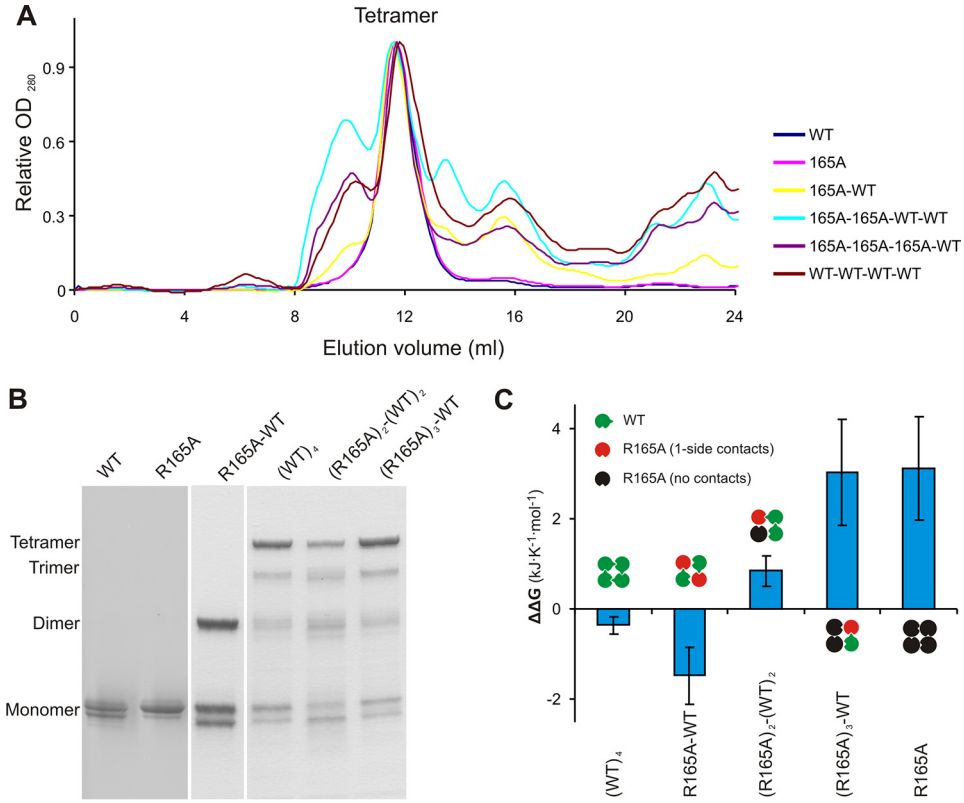

Figure 3. Stoichiometric effect of R165A mutation on PIP_2 sensitivity of KirBac1.1. *A*, gel filtration profiles of affinity-purified KirBac1.1 R165A dimeric or tetrameric tandem proteins. The running buffer for all gel filtration was 20 mM Hepes, 150 mM KCl, 5 mM decyl-maltoside, pH 7.5. *B*, SDS-PAGE of affinity-purified KirBac1.1 mutant proteins with different stoichiometry. *C*, effect of number and location of R165A mutations within the KirBac1.1 tetramer on PIP_2 sensitivity. K_i (the PIP_2 concentration at which 50% of KirBac1.1 rubidium uptake was inhibited) values were obtained by fitting with the Hill equation using Solver tool of Microsoft Excel. $\Delta\Delta G$ was calculated using equation $\Delta\Delta G = RT\ln(K_{i\,R165X}/K_{i\,WT})$.

results suggest that release of even one protomer from the Arg-165-mediated intersubunit interaction impaired PIP_2 sensitivity and release of two or more impaired sensitivity even more so.

The Arg-165-mediated intersubunit contacts stabilized the KirBac1.1 long-closed state

To uncover the kinetic basis of altered PIP_2 sensitivity in R165A mutants, we performed single-channel recordings on purified KirBac1.1 reconstituted into giant liposomes. Consistent with previous reports (15, 22), single WT KirBac1.1 channels exhibited very heterogeneous gating behaviors, with multiple conductance levels (Fig. 4*A*). Openings occur in bursts, each characterized by rapid flickering transitions between multiple conductance levels and separated by prolonged interburst closures (Fig. 4*A*). Although the single-channel conductance profile within the burst did not differ markedly from that of WT, R165A mutant channels exhibited shorter prolonged closures (Fig. 4, *A* and *B*). Detailed kinetic analysis indicates that the R165A mutation did not alter the mean closed time significantly (Fig. 4*F*), but it markedly destabilized the longest closed state (Fig. 4*C*), reducing the interburst duration >8-fold (Fig. 4, *D* and *G*). Consequently, the R165A mutant demonstrated more frequent burst-openings than WT and, therefore, higher P_o (Fig. 4*E*).

The R165A mutation induces structural changes that promote channel opening

We examined the conformational changes in channel structure that are induced in the presence and absence of PIP_2 on the R165A background using a macroscopic FRET approach (12). We introduced cysteine residues at different locations throughout the cytoplasmic domain on the KirBac1.1 R165A background and measured the FRET efficiencies between the fluorophore pair EDANS and DABCYL-plus covalently attached to purified channel proteins reconstituted into liposomes (Fig. 5, Table 1). Eight of 17 fluorophore-labeled cysteine mutants on the R165A background retained high channel activity (Fig. 5*A*), and all exhibited reduced PIP_2 inhibition compared with WT (Fig. 5, *C* and *D*). We previously demonstrated that, on the WT background, the FRET-predicted intersubunit distances of labeled residues significantly correlated with those from the KirBac1.1 crystal structure ($R = 0.71$, $p < 0.001$; Fig. 5*C*) (12), but a weaker correlation was revealed in the KirBac1.1[R165A] mutant ($R = 0.063$, $p < 0.804$; Fig. 5*C*), with predicted Cα-Cα distances being uniformly greater than on the WT background (Fig. 5*D*).

Previously we mapped PIP_2-dependent structural arrangements of WT KirBac1.1 channel in liposomes (12). The results showed that PIP_2 induces rigid body motions of the cytoplasmic domain secondary structures, in particular a decrease in the tilt of the major β-sheet to align closer with the membrane normal, effectively opening the cytoplasmic

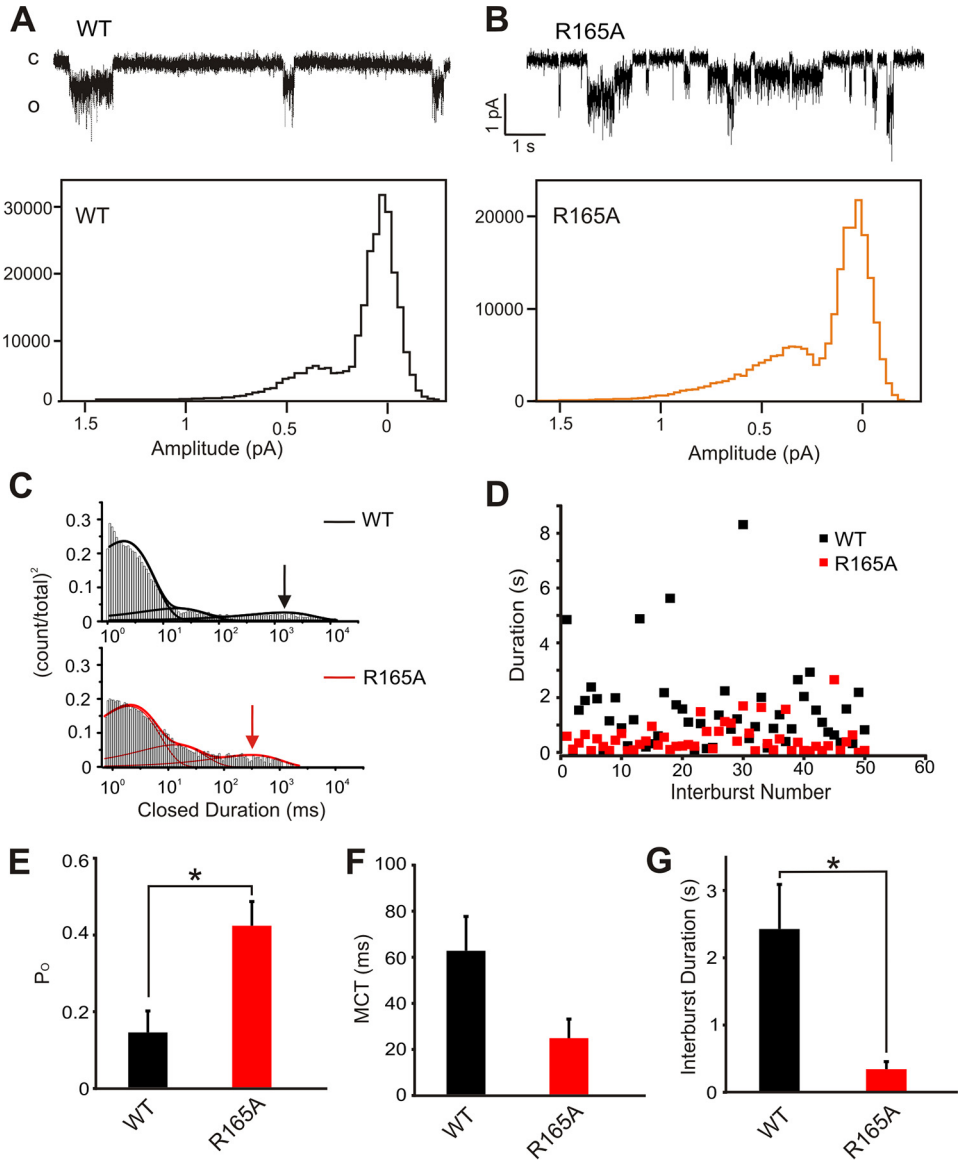

Figure 4. R165A enhanced KirBac1.1 activity by reducing the interburst closed time. *A* and *B*, representative single channel recordings (*above*) and single channel current amplitude histogram (*below*) of purified KirBac1.1 WT and R165A mutant in giant liposomes at +100-mV membrane potential. *C*, closed lifetime histograms overlaid with the probability density function (*thick solid line*) of KirBac1.1 WT and R165A mutant, which were fit well with three exponential components (*overlaid lines*) with the longest component marked by arrows. *D*, distribution of interburst duration of KirBac1.1 WT and R165A from the entire recording depicted in *A* and *B*. *E*, open probability (P_o), mean closed time (*MCT*) (*F*), and interburst duration (*G*) of KirBac1.1 WT and R165A. WT, $n = 4$ patches; R165A, $n = 5$ patches in *E–G*; *, $p < 0.05$.

vestibule (Fig. 6, *C* and *F*). However, in the R165A mutant channel background, the PIP_2-induced conformational changes reported by FRET exhibited very different patterns (Fig. 6, *A* and *D*, Table 1). The major β-sheet still underwent what appears to be a rigid motion, but all residues in the major β-sheet now moved outward from the central axis in the presence of PIP_2 (Fig. 6, *B* and *E*), potentially underlying the failure of PIP_2 binding to promote channel closure in the mutant channel (see "Discussion").

Discussion

Conserved CD-I salt-bridge roles in pro- and eukaryotic Kir channels

All Kir channels share highly conserved structure overall and are all highly sensitive to PIP_2 (7, 19). All eukaryotic Kir channels are activated by PIP_2, whereas KirBac1.1 channels are inhibited. Previous studies (24, 30) show that highly conserved salt-bridge pairs in the interface between cytoplasmic domains (CD-I) reduced apparent PIP_2 sensitivity of eukaryotic Kir channels by stabilizing a PIP_2-inaccessible, inactivated closed state (24). In the present study we show that breaking this intersubunit interaction also reduces apparent sensitivity to PIP_2 in prokaryotic KirBac1.1, resulting in stabilization of a PIP_2-inaccessible open state.

Structural consequences of CD-I disruption

Kir channel crystal structures have demonstrated that there are four binding pockets for PIP_2 in each channel (8, 9), but stoichiometric requirements of PIP_2 for Kir channel gating and the molecular details of intersubunit interactions in coordinat-

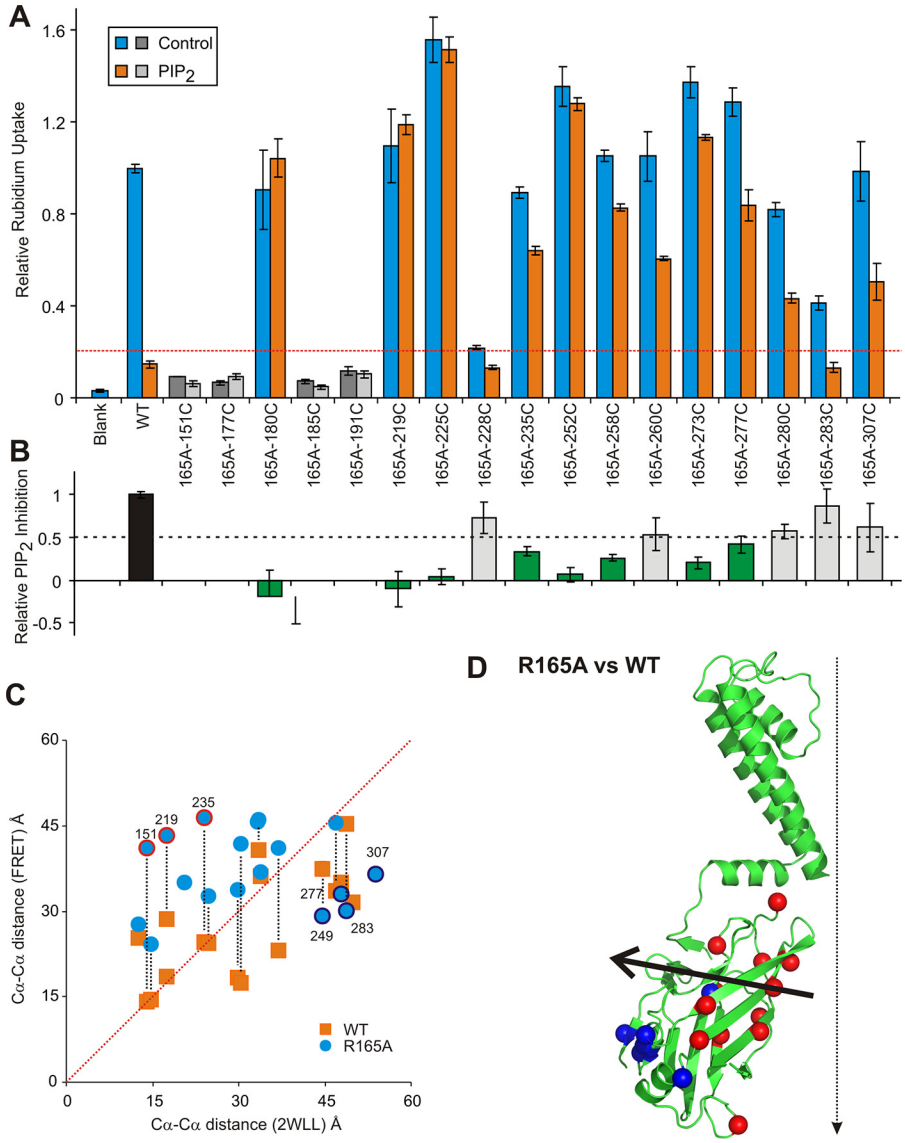

Figure 5. Correlation analysis revealed significant structural changes in KirBac1.1 due to the R165A mutation. *A*, relative rubidium uptake of KirBac1.1 cysteine mutants (on the R165A background) labeled with EDANS/DABCYL-plus (E/D) FRET pairs in the presence and absence of 1% of PIP_2 (mean ± S.E., $n = 3$ in each case). Mutants with substantially lower rubidium uptake than WT (>20%, *gray*) were not analyzed further. *B*, relative PIP_2 inhibition of E/D-labeled KirBac1.1 cysteine mutants on the R165A background. Relative PIP_2 inhibition was calculated from *A* and normalized to WT. All mutants were variably less sensitive than WT (*green*). *C*, Cα-Cα distance between adjacent subunits of labeled residues assessed by FRET *versus* those determined in the KirBac1.1 (PDB code 2WLL) crystal structure. KirBac1.1 cysteine-substituted proteins on the WT or R165A background were purified, labeled, and reconstituted into liposomes (POPE:POPG = 3:1) with or without 1% PIP_2, apparent FRET efficiencies were measured, and Cα-Cα distances were calculated using a tetrameric FRET model as that described previously (12). *D*, schematic illustration of significant structural changes induced by the R165A mutation in KirBac1.1 subunits. The Cα of residues subjected to FRET measurements are highlighted as *spheres*, with those that move toward the pore axis colored *blue* and those that move away colored *red* upon the addition of PIP_2 or introduction of R165A background mutation. The major β-sheet uniformly moves away from the central axis (*arrow*) in the R165A background.

ing PIP_2-induced conformational changes remained unclear. Our results indicate that the existence of even one subunit with zero Arg-165-mediated interactions significantly attenuated PIP_2 sensitivity of the tetrameric KirBac1.1 channel (Fig. 3*C*). Because Arg-165 is located far from the location of PIP_2 binding, the change in PIP_2 sensitivity reflects a long-range consequence of structural disruption and may reflect the requirement for coordination between subunits in channel gating. Compared with WT channels, macroscopic FRET measurements (Fig. 5*A*) reveal a striking increase of apparent intramolecular distances of 10–20 Å at almost all residues in the KirBac1.1[R165A] cytoplasmic domain, suggesting that the R165A mutation leads to a major dilation of the cytoplasmic domain. This dramatic result could be explained by a breaking apart of the CD-I. In this case the PIP_2-binding site, located at the CD-I would be broken and would have to reform for PIP_2 to bind. Consistent with this suggestion, at almost every residue in the major β-sheet, PIP_2 induced a decrease in the predicted intramolecular distances. This is in marked contrast to the findings in the WT background background (12) (Fig. 6), as illustrated by the schematic in Fig. 7.

There are obvious parallels between the CD-I collapsed mechanism we propose and rupture of the ligand-binding domain dimer interface that mediates glutamate receptor desensitization (31). Recent cryo-EM structures of resting, activated, and desensitized glutamate receptor conformations sug-

Table 1
Apparent FRET efficiencies of labeled KirBac1.1 cysteine mutants on R165A background reconstituting in liposomes

Residue	FRET (R165A)	Cα distances between adjacent subunit (Å)		ΔCα-Cα
		1P7B.PDB	FRET	
Cys-151	0.206 ± 0.000	14.0	41.0	−27
Cys-177	0.313 ± 0.000	33.9	36. 9	3
Cys-180	0.190 ± 0.006	30.4	41.8	−11.4
Cys-185	0.372 ± 0.000	20.6	35.0	−14.4
Cys-191	0.450 ± 0.006	24.7	32.7	−8
Cys-219	0.161 ± 0.004	17.5	43.3	−25.8
Cys-225	0.124 ± 0.000	33.3	45.7	−12.4
Cys-228	0.411 ± 0.013	29.9	33.8	−3.9
Cys-235	0.116 ± 0.000	23.9	46.4	−22.5
Cys-249	0.571 ± 0.002	44.6	29.1	15.5
Cys-252	0.204 ± 0.001	36.8	41.1	−4.3
Cys-258	0.722 ± 0.001	14.7	24.2	−9.5
Cys-260	0.620 ± 0.004	12.5	27.8	−15.3
Cys-273	0.120 ± 0.000	33.4	46.0	−12.6
Cys-277	0.439 ± 0.000	47.8	33.0	14.8
Cys-280	0.128 ± 0.000	47.0	45.4	1.6
Cys-283	0.543 ± 0.000	48.7	30.1	18.6
Cys-307	0.324 ± 0.003	53.8	36.5	17.3

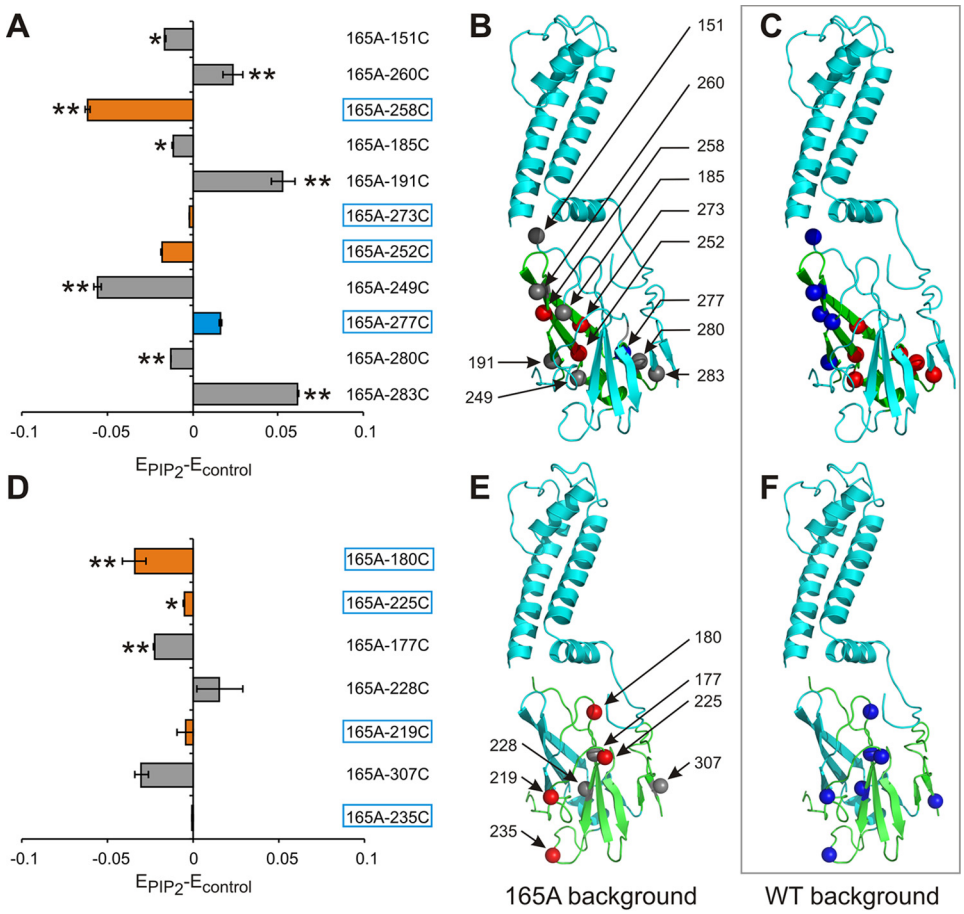

Figure 6. The R165A mutation disrupted PIP_2-induced secondary structural rearrangements. Shown are PIP_2-induced changes of apparent FRET efficiencies ($E_{PIP2} - E_{control}$) of KirBac1.1 cysteine mutants on the R165A background in the large β-sheet (*A* and *B*) and small β-sheets (*D* and *E*). Labeled mutants showing significantly reduced PIP_2 inhibition (from Fig. 4) are highlighted by colors. In *B* and *E*, Cα of the labeled residue is highlighted by *spheres*; residues demonstrating increased FRET efficiency (inward motion) in the presence of PIP_2 are colored *blue*, those demonstrating decreased FRET efficiency (outward motion) are colored *red*; amino acid residues in *panels A* and *D* are listed moving from the membrane surface toward the bottom of the channel. PIP_2-induced structural rearrangements of KirBac1.1 cysteine mutants on the WT background (12) are shown in *panels C* and *F* for comparison, with the same color code as that in *panel B* and *E*. * indicates a significance level for $p < 0.05$, and ** indicates a significance level for $p < 0.01$.

gest that the associated physical motions of domain rearrangements during desensitization are also extensive and involve loss of interface interactions between the ligand-binding domain as well as the amino-terminal domain dimers (32, 33). Two distinct eukaryotic Kir channel cytoplasmic domain conformations are apparent in available crystallographic structures (8, 18). In the absence of PIP_2, the PIP_2-binding site is unstructured, whereas in the presence of PIP_2 the binding site is highly

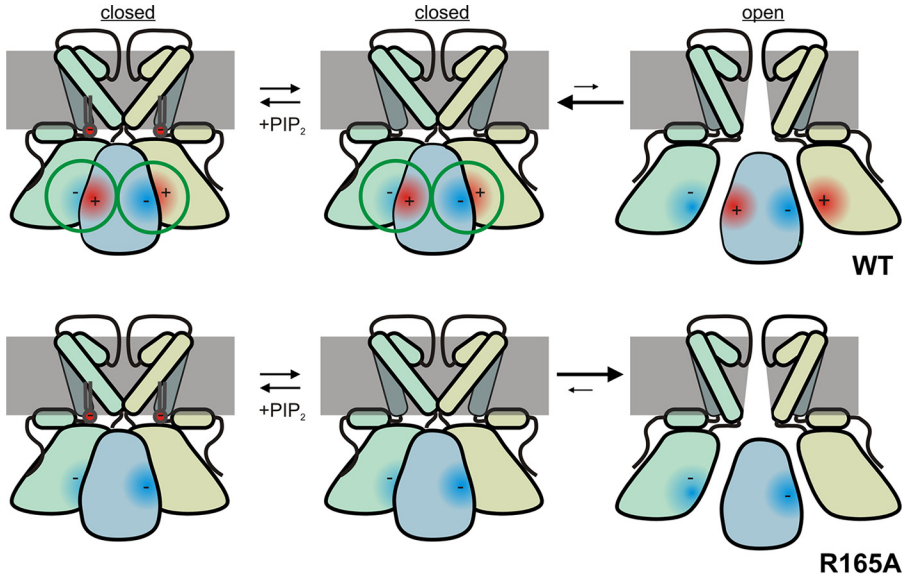

Figure 7. Proposed model of structural and functional role of CD-I salt bridge in Kir channel gating. Shown is a schematic model of KirBac1.1 channel gating. The WT CD-I salt bridge (*circled*) stabilizes the closed state, whereas in the R165A mutant channel, the CD-I is destabilized, and P_o is increased. PIP_2 binds to the "tight" closed state cytoplasmic domain conformation, thereby reducing apparent PIP_2-sensitivity in the R165A mutant channel.

structured, and the whole cytoplasmic domain is pulled closer toward the membrane surface. It is conceivable that the CD-I disrupted and compact configurations are equivalent to the apo (PDB code 3JYC) (18) and PIP_2-bound (3SPI) (8) cKir2.2 structures, respectively. Intersubunit CD-I Cα-Cα distances are longer in the apo configuration, which may, therefore, be favored by mutations that disrupt the salt bridges (Fig. 7), although further experimentation will be required to systematically assess this idea.

Functional consequences of CD-I disruption

Single channel recordings in KirBac1.1 (Fig. 4) demonstrated that the R165A mutation increased the channel P_o by significantly disrupting PIP_2-driven long closures. In eukaryotic Kir channels, the equivalent mutation resulted in decreased channel P_o by inducing a long, PIP_2-inaccessible, closed state (24). Separation of this state from PIP_2-accessible closed states is most obvious in ATP-sensitive (Kir6.2) channels in which the mutation R192A, equivalent to R165A in KirBac1.1, leads to an inactivation phenotype: when ATP is removed, channels open but then rapidly and spontaneously inactivate to a closed state (24, 26). A consistent kinetic model, in which CD-I disruption results in stabilization or appearance of novel inactivated state accessible from the non-PIP_2-bound state can account for inactivation in Kir6.2 and reduced P_o and enhanced PIP_2 sensitivity in Kir2.1 channels (24). By simply assuming that the gating states are opposite in KirBac channels (*i.e.* the PIP_2-stabilized compact CD-I is closed and CD-I disruption stabilizes the open state) the behavior of KirBac1.1 channels are then also readily explained (Fig. 7).

Experimental procedures

DNA manipulation

KirBac1.1 and human Kir2.1 (Kir2.1) mutants in pQE60 or pcDNA3.1 vector were constructed using a site-directed mutagenesis kit (Agilent Inc.) (17); tandem KirBac1.1 dimeric constructs were made by inserting an additional copy of the cDNA between BamHI and HindIII sites of the WT construct, with an intermediate flexible GGGSGGGS linker; two tandem dimers were subcloned into pET-28a(+) vector between NcoI-SacI and SacI-HindIII to make tandem tetrameric constructs.

Protein expression, purification, and labeling

KirBac1.1 was expressed and purified as previously described (17, 34) from BL21-gold(DE3) host cells. For labeling KirBac1.1 cysteine mutants with EDANS c2 maleimide and DABCYL-plus c2 maleimide (E/D, Anaspec), tetrameric fractions from size exclusion chromatography were pooled and concentrated to 1.0 mg/ml, then labeled with an E/D mixture at a protein/E/D ratio of 1:10:10 at room temperature for 1 h. Free fluorophores were then removed by gel filtration. Buffer containing 20 mM HEPES, 150 mM KCl, 5 mM decyl-maltoside, pH 7.5, was used for both labeling and gel filtration.

Rubidium flux assays and FRET measurements

Purified KirBac1.1 proteins were reconstituted into POPE: POPG (3:1) liposomes with or without PIP_2 at a protein/lipid ratio of 1:100. Rubidium flux assays and FRET measurements were performed on proteoliposome samples as described previously (12). For KirBac1.1, relative rubidium uptake of all mutants was normalized against WT protein in liposomes without PIP_2. K_i (PIP_2 concentration inhibiting 50% rubidium uptake) was obtained by fitting with a Hill equation using the Solver tool in Microsoft Excel. Free energy perturbations induced by different mutations on PIP_2 sensitivity of KirBac1.1 ($\Delta\Delta G$) were calculated using the equation,

$$\Delta\Delta G = RT\ln(K_{i\,R165X}/K_{i\,WT}) \quad \text{(Eq. 1)}$$

where R is the gas constant, T is temperature, and $K_{i\,WT}$ and $K_{i\,R165X}$ are the half-inhibitory PIP_2 concentrations for KirBac1.1 WT and mutant, respectively.

Electrophysiology and kinetic analyses

Kir2.1 subunit cDNAs in pcDNA3.1 vector were transiently transfected into COSm6 cells, and excised voltage clamp recordings were performed as described previously (35, 36). Single channel recordings of KirBac1.1 were performed on reconstituted channels in giant liposomes as described (15). Excised inside-out patch clamp recordings were performed with electrodes of 2–5 megaohms and pipette/bath solutions being KMOPS (158 mM KCl, 10 mM MOPS, pH 7.4). Single-channel current responses were measured at ±100 mV, and recordings were low-pass-filtered at 1 kHz, sampled at 10 kHz, and converted into digital files in Clampex7 for offline analysis using QuB kinetic software (QuB software). Recordings were digitally filtered to 0.4 kHz, and single-channel amplitudes were first estimated using the Baum-Welch re-estimation algorithm. Recordings were idealized using a 50% threshold method based on the corresponding single-channel amplitudes, which typically consisted of between 2 and 4 subconductance levels, with no imposed dead time. The corresponding idealization was evaluated for each recording by comparison to that of the unfiltered single-channel activity. State modeling and kinetic analyses were applied to idealized data using a maximum interval log-likelihood (MIL) algorithm (37, 38). A simple linear kinetic model was constructed with the number of closed states based on maximum log-likelihood criteria (10 LL units/state) with an imposed dead time of 900 μs determined by the digital filter frequency to correct for missed events (39). Interburst durations were determined based on the τcrit (critical time) value used to isolate bursts that consisted of >5 opening events and were terminated by closure lasting between 30 and 75 ms as previously described (21).

Data analysis

For correlation analysis, the Cα-Cα distances between labeled residues at adjacent subunits were calculated from measured apparent FRET efficiencies using a tetrameric FRET model described previously (12).

Author contributions—S. W. and C. G. N. conceived the project. S. W. designed the experiments. S. W., W. F. B., S. H., and P. H. performed the experiments and analyzed the data. S. W., W. F. B., and C. G. N. wrote the paper.

References

1. Pattnaik, B. R., Asuma, M. P., Spott, R., and Pillers, D.-A. (2012) Genetic defects in the hotspot of inwardly rectifying K+ (Kir) channels and their metabolic consequences: a review. *Mol. Genet. Metab.* **105,** 64–72
2. Hibino, H., Inanobe, A., Furutani, K., Murakami, S., Findlay, I., and Kurachi, Y. (2010) Inwardly rectifying potassium channels: their structure, function, and physiological roles. *Physiol. Rev.* **90,** 291–366
3. Nichols, C. G. (2006) KATP channels as molecular sensors of cellular metabolism. *Nature* **440,** 470–476
4. Nichols, C. G., Singh, G. K., and Grange, D. K. (2013) KATP channels and cardiovascular disease: suddenly a syndrome. *Circ. Res.* **112,** 1059–1072
5. Tristani-Firouzi, M., and Etheridge, S. P. (2010) Kir 2.1 channelopathies: the Andersen-Tawil syndrome. *Pflugers Arch.* **460,** 289–294
6. Suh, B. C., and Hille, B. (2008) PIP2 is a necessary cofactor for ion channel function: how and why? *Annu. Rev. Biophys.* **37,** 175–195
7. Logothetis, D. E., Jin, T., Lupyan, D., and Rosenhouse-Dantsker, A. (2007) Phosphoinositide-mediated gating of inwardly rectifying K^+ channels. *Pflugers Arch.* **455,** 83–95
8. Hansen, S. B., Tao, X., and MacKinnon, R. (2011) Structural basis of PIP2 activation of the classical inward rectifier K^+ channel Kir2.2. *Nature* **477,** 495–498
9. Whorton, M. R., and MacKinnon, R. (2013) X-ray structure of the mammalian GIRK2-$\beta\gamma$ G-protein complex. *Nature* **498,** 190–197
10. Pegan, S., Arrabit, C., Slesinger, P. A., and Choe, S. (2006) Andersen's syndrome mutation effects on the structure and assembly of the cytoplasmic domains of Kir2.1. *Biochemistry* **45,** 8599–8606
11. Bichet, D., Haass, F. A., and Jan, L. Y. (2003) Merging functional studies with structures of inward-rectifier K^+ channels. *Nat. Rev. Neurosci.* **4,** 957–967
12. Wang, S., Lee, S. J., Heyman, S., Enkvetchakul, D., and Nichols, C. G. (2012) Structural rearrangements underlying ligand-gating in Kir channels. *Nat. Commun.* **3,** 617
13. Lopes, C. M., Zhang, H., Rohacs, T., Jin, T., Yang, J., and Logothetis, D. E. (2002) Alterations in conserved Kir channel-PIP2 interactions underlie channelopathies. *Neuron* **34,** 933–944
14. Xie, L.-H., John, S. A., Ribalet, B., and Weiss, J. N. (2007) Activation of inwardly rectifying potassium (Kir) channels by phosphatidylinositol-4,5-bisphosphate (PIP2): interaction with other regulatory ligands. *Prog. Biophys. Mol. Biol.* **94,** 320–335
15. Cheng, W. W., Enkvetchakul, D., and Nichols, C. G. (2009) KirBac1.1: it's an inward rectifying potassium channel. *J. Gen. Physiol.* **133,** 295–305
16. Kuo, A., Gulbis, J. M., Antcliff, J. F., Rahman, T., Lowe, E. D., Zimmer, J., Cuthbertson, J., Ashcroft, F. M., Ezaki, T., and Doyle, D. A. (2003) Crystal structure of the potassium channel KirBac1.1 in the closed state. *Science* **300,** 1922–1926
17. Enkvetchakul, D., Bhattacharyya, J., Jeliazkova, I., Groesbeck, D. K., Cukras, C. A., and Nichols, C. G. (2004) Functional characterization of a prokaryotic Kir channel. *J. Biol. Chem.* **279,** 47076–47080
18. Tao, X., Avalos, J. L., Chen, J., and MacKinnon, R. (2009) Crystal structure of the eukaryotic strong inward-rectifier K^+ channel Kir2.2 at 3.1 Å resolution. *Science* **326,** 1668–1674
19. Enkvetchakul, D., Jeliazkova, I., and Nichols, C. G. (2005) Direct modulation of Kir channel gating by membrane phosphatidylinositol 4,5-bisphosphate. *J. Biol. Chem.* **280,** 35785–35788
20. D'Avanzo, N., Cheng, W. W., Wang, S., Enkvetchakul, D., and Nichols, C. G. (2010) Lipids driving protein structure? Evolutionary adaptations in Kir channels. *Channels* **4,** 139–141
21. Chakrapani, S., Cordero-Morales, J. F., and Perozo, E. (2007) A quantitative description of KcsA gating II: single-channel currents. *J. Gen. Physiol.* **130,** 479–496
22. Wang, S., Vafabakhsh, R., Borschel, W. F., Ha, T., and Nichols, C. G. (2016) Structural dynamics of potassium-channel gating revealed by single-molecule FRET. *Nat. Struct. Mol. Biol.* **23,** 31–36
23. Bavro, V. N., De Zorzi, R., Schmidt, M. R., Muniz, J. R., Zubcevic, L., Sansom, M. S., Vénien-Bryan, C., and Tucker, S. J. (2012) Structure of a KirBac potassium channel with an open bundle crossing indicates a mechanism of channel gating. *Nat. Struct. Mol. Biol.* **19,** 158–163
24. Borschel, W. F., Wang, S., Lee, S., and Nichols, C. G. (2017) Control of Kir channel gating by cytoplasmic domain interface interactions. *J. Gen. Physiol.* **149,** 561–576
25. Lee, S. J., Ren, F., Zangerl-Plessl, E. M., Heyman, S., Stary-Weinzinger, A., Yuan, P., and Nichols, C. G. (2016) Structural basis of control of inward rectifier Kir2 channel gating by bulk anionic phospholipids. *J. Gen. Physiol.* **148,** 227–237
26. Shyng, S. L., Cukras, C. A., Harwood, J., and Nichols, C. G. (2000) Structural determinants of PIP_2 regulation of inward rectifier K(ATP) channels. *J. Gen. Physiol.* **116,** 599–608
27. D'Avanzo, N., Cheng, W. W., Doyle, D. A., and Nichols, C. G. (2010) Direct and specific activation of human inward rectifier K^+ channels by membrane phosphatidylinositol 4,5-bisphosphate. *J. Biol. Chem.* **285,** 37129–37132

28. Xie, L. H., John, S. A., and Weiss, J. N. (2002) Spermine block of the strong inward rectifier potassium channel Kir2.1: dual roles of surface charge screening and pore block. *J. Gen. Physiol.* **120,** 53–66
29. Clarke, O. B., Caputo, A. T., Hill, A. P., Vandenberg, J. I., Smith, B. J., and Gulbis, J. M. (2010) Domain reorientation and rotation of an intracellular assembly regulate conduction in Kir potassium channels. *Cell* **141,** 1018–1029
30. Lin, Y. W., Jia, T., Weinsoft, A. M., and Shyng, S. L. (2003) Stabilization of the activity of ATP-sensitive potassium channels by ion pairs formed between adjacent Kir6.2 subunits. *J. Gen. Physiol.* **122,** 225–237
31. Kumar, J., and Mayer, M. L. (2013) Functional insights from glutamate receptor ion channel structures. *Annu. Rev. Physiol.* **75,** 313–337
32. Dürr, K. L., Chen, L., Stein, R. A., De Zorzi, R., Folea, I. M., Walz, T., Mchaourab, H. S., and Gouaux, E. (2014) Structure and dynamics of AMPA receptor GluA2 in resting, pre-open, and desensitized states. *Cell* **158,** 778–792
33. Meyerson, J. R., Kumar, J., Chittori, S., Rao, P., Pierson, J., Bartesaghi, A., Mayer, M. L., and Subramaniam, S. (2014) Structural mechanism of glutamate receptor activation and desensitization. *Nature* **514,** 328–334
34. Wang, S., Alimi, Y., Tong, A., Nichols, C. G., and Enkvetchakul, D. (2009) Differential roles of blocking ions in KirBac1.1 tetramer stability. *J. Biol. Chem.* **284,** 2854–2860
35. Kurata, H. T., Cheng, W. W., Arrabit, C., Slesinger, P. A., and Nichols, C. G. (2007) The role of the cytoplasmic pore in inward rectification of Kir2.1 channels. *J. Gen. Physiol.* **130,** 145–155
36. Kurata, H. T., Marton, L. J., and Nichols, C. G. (2006) The polyamine binding site in inward rectifier K^+ channels. *J. Gen. Physiol.* **127,** 467–480
37. Qin, F. (2004) Restoration of single-channel currents using the segmental k-means method based on hidden Markov modeling. *Biophys. J.* **86,** 1488–1501
38. Qin, F., Auerbach, A., and Sachs, F. (1997) Maximum likelihood estimation of aggregated Markov processes. *Proc. Biol. Sci.* **264,** 375–383
39. Qin, F., Auerbach, A., and Sachs, F. (1996) Estimating single-channel kinetic parameters from idealized patch clamp data containing missed events. *Biophys. J.* **70,** 264–280

Conformational changes at cytoplasmic intersubunit interactions control Kir channel gating

Shizhen Wang, William F. Borschel, Sarah Heyman, Phillip Hsu and Colin G. Nichols

J. Biol. Chem. 2017, 292:10087-10096.
doi: 10.1074/jbc.M117.785154 originally published online April 26, 2017